Improving Tactile Feedback with an Impedance Adapter

Jack Lindsay* University of Washington
Richard J. Adams† Barron Associates Inc.
Blake Hannaford‡ University of Washington

ABSTRACT

Vibration motors are often used to generate tactile effects by exciting a mass at a given frequency and amplitude. The characteristic impedance of this vibrotactile device is not always in harmony with the impedance of the human skin. This impedance mismatch can result in poor energy transfer, necessitating larger motors and greater power consumption than otherwise required. Herein, we investigate the feasibility of improving the energy transfer by placing a medium between the skin and the motor, which we dub an impedance adapter. We simulate the effects of this impedance adapter using a mathematical model, and evaluate its effect on skin displacement and a parameter we call skin stimulus. Skin stimulus is introduced as a measure of the perceptive effects of a haptic system, and is used to compare results between systems with an impedance adapter and those without. Our findings suggest a factor of four improvement in skin displacement and a two-fold increase in skin stimulus are possible by introducing an optimized impedance adapter.

1 INTRODUCTION

Vibrotactile devices are commonplace in haptic applications. These devices are often small motors with oscillating or eccentric masses designed to generate perceptible vibrations in a user's skin. The magnitude of the resulting skin displacement must exceed a threshold at an appropriate frequency to produce recognizable haptic effects [18]. Commercially-available motors are typically designed for use in a specific product (such as the buzzer in a smart phone), and may not be optimally suited for a new application that involves an alternate placement and loading conditions. In the most common applications, vibrotactile simulus frequency appears to be designed to stimulate the peak in human sensitivity recorded at about 250Hz [15].

In this paper, we investigate whether or not it is possible to improve the transmission of energy from the device to the skin by introducing a medium between the skin and the motor. This medium would work by adapting the output of the vibration motor to the impedance of human skin. For this purpose, we dub the medium an impedance adapter. How will changes in the characteristics of an impedance adapter have an effect on the deformation of skin? The skin is highly non-linear, and its elasticity shows a non-linear dependence on contact area [18], indentation [5], frequency [10], and location on the body [9]. Practical design constraints make it impossible for a given tactile device to be optimized over all of these variables. However, a simple device placed between the actuator and the skin contact point might effectively match the impedance between the load and source to maximize the power transfer. The efficacy of this device can be measured by its effect on signal amplitude, in this case the stimulus delivered to the skin, and its latency, or the time delay between the signals transmission and its maximum steady-state value.

*jackICL@uw.edu
†adams@barron-associates.com
‡blake@uw.edu

IEEE World Haptics Conference 2013
14-18 April, Daejeon, Korea
978-1-4799-0088-6/13/$31.00 ©2013 IEEE

This paper investigates how an impedance adapter can be tuned to maximize skin deformation in a system driven by a particular class of vibrational motor, a linear resonant actuator (LRA). Furthermore, it considers how variations in the skin model will influence deformation. The LRA was chosen for its low latency and positive response to increases in mass [11]; as well as its low-cost, wide availability, and extensive use in the marketplace. Linear resonant actuators use a voice coil to generate an electrodynamic force between an outer housing and a permanent magnet-mass riding on a spring suspension. By oscillating the electric field, the inner mass vibrates at an amplitude that is a function of the excitation frequency. Maximum amplitude is acheived when the field excitation matches the resonant frequency of the mechanical spring-mass system. An LRA can be designed to produce either normal or tangential displacements, depending on the orientation of the mass and spring. Work by [2] found that the fingerpad is more sensitive to normal forces than tangential forces, as a result of the nearly five-fold greater stiffness in the tangential direction. Therefore systems working on the fingerpad and limited by peak force will see the best results with stimulation normal to the finger[2]. Because we aim to maximize stimulus to the fingerpad, only normal forces are considered in this study.

Skin's mechanical impedance depends on contact area, location on the body, frequency, and direction of displacement. In particular, these parameters influence the reactance, or the contribution of the mass and elasticity. Franke [4] found mass to dominate elasticity over 50 Hz on the thigh, and found it increases with the third power of the contactor diameter. Moore and Mundy [10] found that mass dominates in the range of 130 Hz on the finger pad, and elasticity dominates above 250 Hz or below 80 Hz for a range of contactor areas while damping was nearly constant over the range of frequencies. Wiertlewski and Hayward [19] found stiffness, damping, and mass to follow a roughly 1/3 power law of contactor area on the fingertip when a tangential force was applied, and described the fingertip as a visco-elastic medium with a corner frequency around 100 Hz, above which damping dominated. Lundstrom [9] also found the damping to be nearly constant, both over a range of frequencies and over the surface of the human hand when a normal displacement was applied. Values for stiffness and damping varied widely from study to study, and variation appears to depend on probe area, depth of indentation, frequency, and subject to subject variation [12, 9, 10, 4, 2]. While the lack of consensus in these findings presents challenges for modeling and simulation, we have endeavored to employ the best data available, and make the process transparent such that future work might improve upon our model.

A mechanical model of the human finger does not directly predict the stimulus provided by a haptic device. Previous studies have attempted to quantify the effect of contactor area on "skin stimulus", defined as displacement multiplied by area [11]. These results were based on data taken from the thigh, and cannot be accurately translated to other locations on the body, such as the finger pad [10]. Furthermore, these studies have primarily looked at area versus displacement, with the implicit assumption that the number of mechanoreceptors stimulated by a probe is a linear function of contact area. The relationship is in fact non-linear as a result of overlapping receptive fields and the finite number of mechanoreceptors on the finger[17]. Even a small point will contact a large number of receptors, and increasing the diameter of that point from $0.5mm$

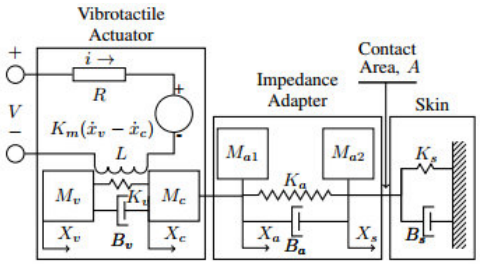

Figure 1: Dynamic model of vibrotactile actuator coupled to skin with an impedance adapter. Skin parameters depend on many variables including contact area (see text).

to 2*mm* has almost no effect on the number of receptors stimulated. Similarly, because of the finite size of the fingerpad, decreasing the tactile devices diameter from the full width of the fingerpad to a diameter approximately four millimeters smaller should stimulate nearly the same number of tactile receptors, albeit at the edge of their receptive fields. These factors must be considered if total skin stimulus is to be properly quantified.

Even significant stimulus can be hamstrung by time lag. Perceived latency between an event and the onset of vibrotactile stimulus can degrade the quality of feedback, but only begins to make an impact on user error rates beyond 25ms, and is not significantly perceptable until 50 ms of lag [8, 1]. Therefore, in circumstances where user error is unacceptable, design of an impedance adapter should result in effective latencies of less than 25 ms. Likewise, in circumstances where some user error is acceptable, but perception of lag is not, latency should be constrained to within 50 ms. The addition of a transmission medium has the capacity to increase latency by delaying the signal from the motor and the success of the impedance adapter requires that it not increase latency beyond thresholds for error rate. As we investigate how a transmission medium can match a signal to the impedance of the skin, we will give special attention to delays in time to perception.

The design of high bandwidth low-profile tactile feedback systems demands optimization with respect to user perception of tactile sensation. Maximizing skin stimulus requires balancing skin indentation with stimulation of a large number of receptors. No known previous work has quantified the optimal balance between indentation and the number of receptors stimulated, an important component in the engineering of high-performance tactile systems.

2 Methods

2.1 Model

A mechanical model of the complete system comprising the LRA, impedance adapter, and finger was built using the standard system diagram approach (Figure 1). The modeling of the actuator came directly from analysis of the components of a C10-100 LRA (Precision Micro Drives[7], London, UK). The finger model is based on analysis of the literature reviewed in table 1. The impedance adapter is idealized as two masses, one connected to the LRA, the other to the skin, with a spring and damper between them.

The impedance adapter is modeled by four parameters, M_{a1}, M_{a2}, K_a, and B_a, describing the mass attached to the LRA, the mass attached to the skin, the spring between these two masses, and the damping between these two masses. The skin is modeled by a stiffness, K_s, and a damping, B_s. Contact area, A, governs changes in the skin impedance as described above.

This model produces the following equations of motion:

$$L\dot{i} + iR + K_m(\dot{x}_a - \dot{x}_v) = v(t) \tag{1}$$

$$M_v\ddot{x}_v + B_v(\dot{x}_v - \dot{x}_a) + K_v(x_v - x_a) = -K_m i \tag{2}$$

$$\begin{aligned}(M_c + M_{a1})\ddot{x}_a + B_v(\dot{x}_a - \dot{x}_v) + B_a(\dot{x}_a - \dot{x}_s) \\ + K_v(x_a - x_v) + K_a(x_a - x_s) = 0\end{aligned} \tag{3}$$

$$M_{a2}\ddot{x}_s + B_a(\dot{x}_s - \dot{x}_a) + K_A(x_s - x_a) + K_s x_s + B_s\dot{x}_s = 0 \tag{4}$$

These equations of motion produce the following linear first-order system of equations of the form $\dot{x} = Ax + Bu$ where

$$A = \begin{bmatrix} \frac{-R}{L} & 0 & \frac{K_m}{L} & 0 \\ 0 & 0 & 1 & 0 \\ \frac{-K_m}{M_v} & \frac{-K_v}{M_v} & \frac{-B_v}{M_v} & \frac{K_v}{M_v} \\ 0 & 0 & 0 & 0 \\ \frac{K_m}{M_{cl}} & \frac{K_v}{M_{cl}} & \frac{B_v}{M_{cl}} & \frac{-(K_a+K_v)}{M_{cl}} \\ 0 & 0 & 0 & 0 \\ 0 & 0 & 0 & \frac{K_a}{M_{a2}} \end{bmatrix}_{Cols 1-4}$$

$$\begin{bmatrix} \frac{-K_m}{L} & 0 & 0 \\ 0 & 0 & 0 \\ \frac{B_v}{M_v} & 0 & 0 \\ 1 & 0 & 0 \\ \frac{-(B_a+B_v)}{M_{cl}} & \frac{K_a}{M_{cl}} & \frac{B_a}{M_{cl}} \\ 0 & 0 & 1 \\ \frac{B_a}{M_{a2}} & \frac{-(K_a+K_s)}{M_{a2}} & \frac{-(B_a+B_s)}{M_{a2}} \end{bmatrix}_{Cols 5-7} \tag{5}$$

$$x = \begin{bmatrix} i & x_v & \dot{x}_v & x_a & \dot{x}_a & x_s & \dot{x}_s \end{bmatrix}^T, \tag{6}$$

$M_{c1} = M_c + M_{a1}$, $B = [1/L, 0, 0, 0, 0, 0, 0]^T$, and $u = [V_{in}, 0, 0, 0, 0, 0, 0]^T$.

The csim() utility in Scilab[13] was used to simulate the time response of this system to sinusoidal inputs. The input to the system had an amplitude of 5V (10V peak-to-peak) and a frequency of 225Hz. For the purposes of this investigation we focused on the steady state root-mean-squared (RMS) value of x_s, the displacement of the skin. M_{a1}, M_{a2}, K_a, and B_a, and contact area, A, were then optimized (by a numeric search described below) to maximize steady state RMS skin displacement.

Parameters for the system (Table 1) were chosen based on values in the literature or the relevant manufacturer's data sheet [7] and verified by experiment where possible. Masses were found by disassembling a device and weighing its components. The resistance was measured using a multimeter. The elasticity, damping, and motor constant of the LRA were derived from its impulse response, which was measured by dropping the LRA and recording its voltage output response on an oscilloscope. Parameters were identified by fitting a damped exponential function with complex poles to this response constrained by the otherwise known values of mass, M_v, M_c, and resistance, R. Parameters for the impedance adapter were tuned through a numerical search and will be discussed in the results section.

To simulate the finger we chose to set a minimum value of skin stiffness at $600N/m$ and a maximum at $2000N/m$, both well within the reported range, and specific skin stiffness was set as a function of a 1/3 power of contact area between those two extremes. Likewise, we set the minimum value for damping at 0.75 $Nsec/m$ and the maximum at 2.38 $Nsec/m$, values which lay within the reported range, and set specific damping as a function of a 1/3 power of area. Variation across the human population was not accounted for.

A brute force numerical search was performed over the four parameters of the impedance adapter (M_{a1}, M_{a2}, K_a, B_a and A) to find

Parameter	Value	Source
L	$130uH$	C10-100 Actuator Datasheet
R	27Ω	Measured, Data Sheet
M_v	$1.4g$	Measured, Data Sheet
M_c	$0.6g$	Measured, Data Sheet
B_v	$0.0322Nsec/m$	Experiment
K_v	$2800N/m$	Experiment
K_m	$1.0N/A$	Experiment
K_s	600-1200N/m	[10, 9, 2, 19, 16, 14]
B_s	0.75-2.38 $Nsec/m$	[10, 9, 19]

Table 1: Model Parameters

Parameter		Parameter Search Range
M_{a1}	Mass attached to motor case	0.25 - 10.0g
M_{a2}	Mass attached to skin	0.25 - 10.0g
K_a	Impedance adapter spring	2000 - 12000 N/m
B_a	Impedance adapter damping	0.01 - 0.1 $Nsec/M$
A	Contact area	1 - 100 mm^2

Table 2: Parameter search ranges for the impedance adapter parameters.

the greatest steady state RMS skin displacement for a fixed input. Ranges for each parameter (Table 2) were established through a preliminary study that quantified the impact of individual parameter variations on system response. Parameters were then assigned limited ranges in which their impact on performance was non-negligible. In some cases the search returned results at either end of the range, indicating that an optimum may lie outside an achievable value. In these circumstances ranges were adjusted within physical limitations of the basic design. For instance, contact area was constrained to an upper bound the approximate size of the fingerpad and a lower bound designed to prevent skin puncture with a sharp, needle-like area. Likewise, masses were kept above 10 percent of the motor's mass to ensure they were manufacturable, and damping was constrained to a minimum value of $0.01Ns/m$ because it cannot be entirely eliminated from physical designs. Each parameter was given 20 values within its search range.

The final performance measure we consider is skin stimulus. Evaluating skin stimulus requires an understanding of how increasing the depth of indentation and the number of mechancoreceptors stimulated impacts afferent nerve response. Mechanoreceptor response has a non-linear dependance on depth of indentation [6], and psychophysical sensation is non-linear as well, though the non-linearites do not appear to be correlated [17]. Importantly, both the mechanoreceptor response and psychophysical sensation appear to be linear at low indentations ($< 0.5mm$) [17]. Therefore stimulation can be considered proportional to indentation at small amplitudes. Furthermore, the responses of a population of receptors is additive [6]. Thus a representative skin stimulus parameter, S, can be defined as:

$$S = N_r \times x_{sRMS} \tag{7}$$

where N_r is the number of receptors and x_{sRMS} is the depth of skin indentation. Both the number of receptors stimulated and the depth of indentation are functions of contact area. Increasing contact area increases the number of receptors a device will directly stimulate. At the same time, for a constant input, increasing contact area reduces the depth of indentation. Therefore Eqn. 7 can be used to find the approximately optimal contact area to deliver vibrotactile stimulus to the fingerpad.

To determine the number of receptors directly stimulated by a device, the receptive fields on the fingerpad are modeled by a grid of overlapping circles whose radii define the receptive fields. The fingerpad is populated by four different types of mechanoreceptors;

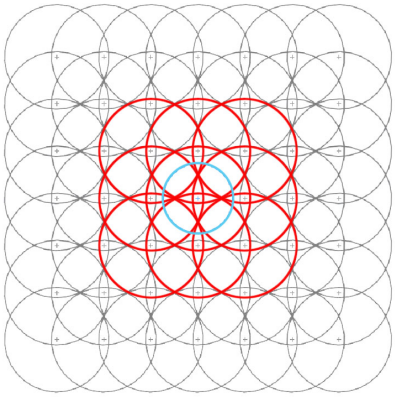

Figure 2: Receptive fields on the fingerpad. The blue cicle represents a contactor of radius 2, the red circles represent those receptors directly stimulated, and the grey circles are those unaffected.

Contact condition	Area	x_{sRMS}
LRA direct	$78.5mm^2$	0.0438mm
LRA with cone	$1.0mm^2$	0.0455mm
LRA with Impedance Adapter	$1.0mm^2$	0.1917mm

Table 3: Steady state RMS displacement with sinusoidal 5V input under three contact conditions.

however, only fast acting type 2 (FAII) receptors are highly receptive to vibrations around 250Hz [17]. Valbo and Johansson found FAII mechnoreceptors to have receptive fields of approximately 101 mm^2. Thus $5.7mm$ was used as the radius for the receptive fields. FAII receptors have an innervation density of approximately $0.22/mm^2$ on the fingerpad[17]; this was the density used in simulation. Coupling this data with a model of a human fingerpad that is $15mm \times 15mm$ produces a grid of overlapping circles with $5.7mm$ radii across a space $15mm \times 15mm$. Simulated contactors with radii from $1mm$ to $7.5mm$ were then placed in the center of this system and the number of FAII receptive fields contacted for each contactor radius was recorded. This provided a measure of the number of FAII receptors directly stimulated over a range of contact areas. [3] found that additional mechanoreceptors can be stimulated by waves propogating through the body; careful analysis of the magnitude of these distant vibrations is beyond the scope of this paper. We submit this current means of measuring skin stimulus as an approximate measure.

3 Results

3.1 Initial Simulation

First, the model was simulated without an impedance adapter present. There are two relevant cases. One, the LRA can be applied directly in contact with the skin. The device we used had a surface area of $78.5mm^2$ which was thus a fixed parameter in the model. The resulting steady state RMS displacement was $0.0438mm$ (Table 3). Two, a rigid massless cone could be placed between the LRA and the skin, reducing the stimulation area to 1 mm^2. In this case, the resulting steady state RMS displacement was $0.0455mm$

When driven by the 10V peak-to-peak sinusoid described above, the current and power computed at the electrical input were 130 mA and 457 mW in the steady state. The phase angle between voltage and current was 0.1 degrees.

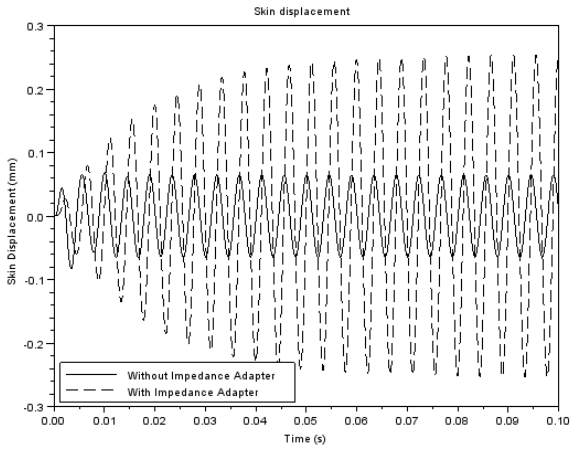

Figure 3: Simulated skin displacement over time. The system with an impedance adapter has a much longer rise time, but achieves an amplitude approximately four times greater than the system without.

Parameter		Optimal value
M_{a1}	Mass attached to motor case*	$0.25g$
M_{a2}	Mass attached to skin	$4.35g$
K_a	Impedance adapter spring	$8200N/m$
B_a	Impedance adapter dampin*g	$0.01Nsec/M$
A	Contact area*	$1.0mm^2$
ω_d	Resonant frequency	$218Hz$

Table 4: Optimized impedance adapter parameters. Values marked with * were saturated at their lower search bound.

3.2 Optimization for skin displacement

The numerical search described above produced parameters that maximized steady state RMS skin displacement in response to the sinusoidal +/-5V input to the LRA. The process yielded a steady state RMS skin displacement 4.4 times larger than the displacement without an impedance adapter, and reduced RMS current consumption and power by 15%. A plot of skin displacement over time for both the system with an impedance adapter and without are shown in Figure 3. The parameters of the optimized impedance adapter are shown in Table 3.

Some of these parameters proved to be sensitive to small changes, while others were more robust. In particular, changes made to the mass attached to the skin (M_{a2}), the impedance adapter stiffness (K_a), and the skin damping (B_s) resulted in large changes in the steady state RMS displacement of the skin (Figure 4). Parameters not shown (M_{a1}, B_a, and K_s) impacted the output by less than 2 percent when varied by up to 50 percent.

3.3 Skin Stimulus

By geometric analysis, we computed the number of mechanoreceptors stimulated as a function of contactor area (Figure 5). These data were then combined with results from the LRA-Impedance adapter model, which supplied the steady state RMS depth of indentation for contactors of any given area. The two sets of data were combined according to Equation 7, and the results are plotted below in Figure 6. The maximum skin stimulus possible with an impedance adapter was 4.90, while the maximum stimulus without an adapter was 2.15 (both in units of $mm \times N_r$). The system with an impedance adapter achieved greater than twice the stimulus of the system without.

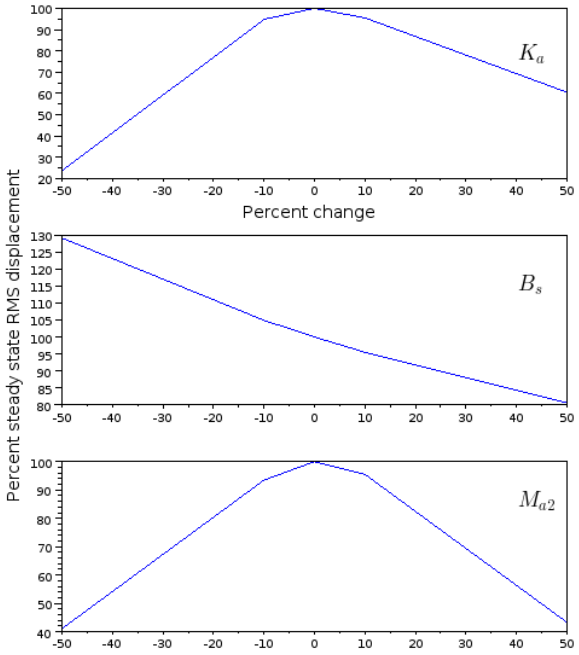

Figure 4: Sensitivity of RMS displacement output to changes in the impedance adapter and the skin model parameters. K_a impedance adapter stiffness; B_s skin damping; M_{a2} mass at skin contact. X-axis: percent change from optimal parameter value, Y-axis: relative steady state RMS displacement.

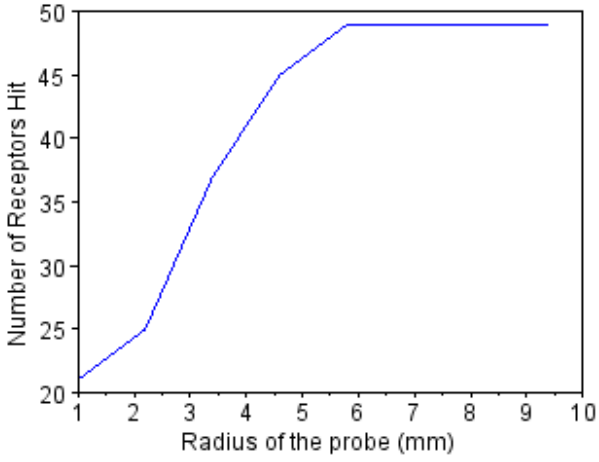

Figure 5: Number of receptors stimulated (N_r) as a function of contactor area.

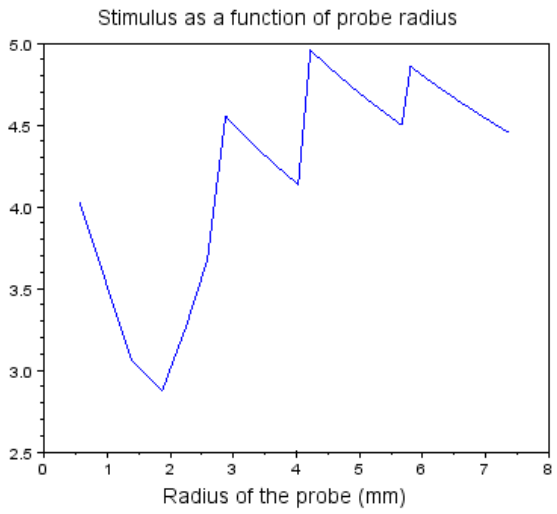

Figure 6: Skin Stimulus as a function of contactor radius. The rough contours of the graph are an artifact of simulation due to a simplified distribution of skin receptors.

4 Discussion and Conclusions

Our simulations of a vibrotactile actuator, impedance adapter, and skin showed that an impedance adapter could increase the steady state RMS displacement of the skin by a factor of 4.4, and the total skin stimulus by a factor of 2.3. These improvements reflect the increased transmission of energy from the actuator through the skin, facilitated by the mechanical properties of the impedance adapter. The presence of a tuned impedance adapter improves signal transmission, increasing energy input to the skin while simultaneously decreasing energy consumed by the motor. These results show the potential of an impedance adapter to improve haptic feedback and lower power consumption in haptic devices.

The simulation of receptor fields (Figures 2, 5, and 6) did not account for the gradual drop off in the receptive field of FAII type mechanoreceptors, and simply used the average field size given in the literature for the human fingerpad [17]. It is not known exactly how far these fields extend, and they appear to be subject to great variability[17]. We restricted our model to be within the demonstrated range of these receptors, and produced a conservative estimate. This platonic model simulated a finger where all the receptors are evenly spaced, and all have an equally large fields with sharp edges. The sharp changes in stimulation depicted in Figure 6 occur when the increased radius makes it just barely possible to reach the edge of a receptors receptive field. In reality we would expect more gradual shifts in skin stimulus owing to the variable distribution of receptors and receptive fields which drop off slowly, thus smoothing the jagged edges in Figure 6. Nevertheless, the results highlight a trade-off between smaller indentation and increased quantity of receptors stimulated as probe size is increased.

Conflicting reports in the literature make it difficult to develop a model of the human fingerpad that could be said to be accurate for all people in all cases. Furthermore, between subjects variation was great enough in some studies to substantially influence the absolute amplitude of vibration found in our model [19]. Better models of the skin's mechanical properties over a range of factors such as contact area and depth of indentation will help refine this work, and are necessary to ground the results of the simulation in the real world. Nonetheless, the model can provide concrete information on the design of a real-world impedance adapter. For example, the model supports the existance of an optimum value for impedance adapter stiffness and showed that damping in the impedance adapter should always be minimized.

The optimization set a lower limit on contact area, damping, and M_{a1} at 1 mm^2, 0.01 Ns/m, and 0.25 g, respectively. As Table 2 makes clear, these were also their final optimized values. If unconstrained, these values would go to zero. Damping is a measure of energy the system can absorb. In this case, were trying to maximize energy transmission, so lowering the damping makes sense. Likewise, contact area was used in a 1/3 power law to find skin stiffness and damping. As contact area shrinks, so does skin stiffness and damping, both factors which impede contactor displacement. Therefore it makes sense for the optimization to shrink these values to their minimum.

The mass attached to the LRA, M_{a1}, is the third variable driven to zero in our numerical search. In parametric analysis where the value of M_{a1} is varied while all other parameters were held constant, its effect on steady state displacement is almost non-existent when it remains below 2 grams. Beyond this point it seems to cause a steady decrease in steady state displacement until it reaches 25 grams, the limit of the test. These tests show that decreasing M_{a1} below 2 grams results in marginal increases in displacement. Should a constraint such as manufactuability require M_{a1} to be an order of magnitude greater than the optimium value, the performance penalty will be small.

The introduction of an impedance adapter did not increase the latency of the system. As figure 3 shows, both systems followed the same curve at the start of the stimulus, and there was no point when the system without an impedance adapter produced a larger displacement. Thus the system with an impedance adapter had an equivalent time to perception. To the extent the model is linear, an input voltage one third the size will produce an output displacement one third as large. This opens the door to very low power vibrotactile systems which use an impedance adapter to achieve equivalent displacement while cutting power. However, these systems may face a much greater latency as a system with an impedance adapter has a much longer rise time than a system without.

Furthermore, these systems may suffer from non-linear effects in the skin, the motor, and the mode of operation. As previously discussed, the dynamics of the skin are highly non-linear. We have attempted to include some non-linearity into our model by defining the skin parameters as a function of a 1/3 power law of area, and avoid other areas of non-linearity by indenting the skin by only a few hundred microns, but these fixes do not insulate our model from error in the skin mechanics. Likewise, our system does not capture the real-world non-linearity of the LRA, which has travel limits on its moving mass and a spring that is likely to be non-linear near those limits. Finally, the model does not account for discontinous contact between the impedance adapter and the skin. These effects are sure to play a role, and require experimental verification.

Conclusion

This paper demonstrates that an optimized mass-spring-damper, dubbed an impedance adapter, placed between a vibrational actuator and the human skin can potentially increase skin displacement, and thus the magnitude of the resulting haptic stimulus. An impedance adapter provides a means to significantly improve haptic feedback by matching the impedance of the signal to the impedance of the source. Simulations based on a commonly available linear resonant actuator (LRA) demonstrate that such a device could increase skin displacement by a factor of four, and double skin stimulation. Future work will explore development and testing of functional impedance adapters to reduce the size and cost of traditional vibrotactile systems, and allow for their use in a wider array of applications. Furthermore, improvements in the understanding of traveling vibrotactile waves could help to improve the optimization of skin stimulus, and should be explored.

ACKNOWLEDGEMENTS

We are pleased to acknowledge support from NASA via an SBIR grant to Barron Associates.

REFERENCES

[1] B. Adelstein, D. Begault, M. Anderson, and E. Wenzel. Sensitivity to haptic-audio asynchrony. *Proceedings of the 5th international conference on Multimodal interfaces*, pages 73–76, 2003.

[2] J. Biggs and M. Srinivasan. Tangential versus normal displacements of skin: Relative effectiveness for producing tactile sensations. *Haptic Interfaces for Virtual Environment and Teleoperator Systems, 2002. HAPTICS 2002. Proceedings. 10th Symposium on*, pages 121–128, 2002.

[3] B. Delhaye, V. Hayward, P. Lefèvre, and J. Thonnard. Texture-induced vibrations in the forearm during tactile exploration. *Frontiers in Behavioral Neuroscience*, 6, 2012.

[4] E. Franke. Mechanical impedance of the surface of the human body. *J. Appl. Physiology*, 3:582–590, 1951.

[5] M. Fritschi, K. Drewing, R. Zopf, M. Ernst, and M. Buss. Construction and first evaluation of a newly developed tactile shear force display. In *Proceedings of the 4th International Conference EuroHaptics 2004*, pages 508–511, 2004.

[6] A. Goodwin and H. Wheat. Physiological mechanisms of the receptor system. *Human Haptic Perception: Basics and Applications*, pages 93–102, 2008.

[7] P. M. D. Inc. Website. *http://precisionmicrodrives.com*, 2012.

[8] C. Jay, M. Glencross, and R. Hubbold. Modeling the effects of delayed haptic and visual feedback in a collaborative virtual environment. *ACM Transactions on Computer-Human Interaction (TOCHI)*, 14(2):8, 2007.

[9] R. Lundström. Local vibrationsmechanical impedance of the human hand's glabrous skin. *Journal of biomechanics*, 17(2):137–144, 1984.

[10] T. Moore and J. Mundie. Measurement of specific mechanical impedance of the skin: effects of static force, site of stimulation, area of probe, and presence of a surround. *The Journal of the Acoustical Society of America*, 52:577, 1972.

[11] B. Mortimer, G. Zets, and R. Cholewiak. Vibrotactile transduction and transducers. *The Journal of the Acoustical Society of America*, 121(5):2970–2977, 2007.

[12] D. Pawluk, R. Howe, et al. Dynamic lumped element response of the human fingerpad. *Journal of biomechanical engineering*, 121(2):178, 1999.

[13] Scilab. Website. *http://www.scilab.org*, 2012.

[14] E. Serina, C. Mote, and D. Rampel. Mechanical properties of the fingertip pulp under repeated, dynamic, compressive loading. volume 31, pages 245–246. AMERICAN SOCIETY OF MECHANICAL ENGINEERS, 1995.

[15] K. Shimoga. A survey of perceptual feedback issues in dexterous telemanipulation. I. finger force feedback. In *Proceedings IEEE VRAIS-93*, pages 263–70, Seattle, WA, Sept. 1993.

[16] M. S. T.T. Diller, D. Schloerb. Frequency response of human skin in vivo to mechanical stimulation. Technical Report 648, MIT Research Laboratory of Electronics (RLE), Feb. 2001.

[17] Å. Vallbo, R. Johansson, et al. Properties of cutaneous mechanoreceptors in the human hand related to touch sensation. *Human neurobiology*, 3(1):3–14, 1984.

[18] R. Verrillo. Vibrotactile thresholds for hairy skin. *Journal of Experimental Psychology; Journal of Experimental Psychology*, 72(1):47, 1966.

[19] M. Wiertlewski and V. Hayward. Mechanical behavior of the fingertip in the range of frequencies and displacements relevant to touch. *Journal of biomechanics*, 45(11):1869–1874, 2012.